Functional analysis of the three major PGRPLC isoforms in the midgut of the malaria mosquito Anopheles coluzzii

Faye H. Rodgers, Julia A. Cai, Andre N. Pitaluga, Dominique Mengin-Lecreulx, Mathilde Gendrin, George K. Christophides

HAL Id: hal-02389245
https://hal.science/hal-02389245

Submitted on 13 Nov 2020

Functional analysis of the three major PGRPLC isoforms in the midgut of the malaria mosquito *Anopheles coluzzii*

Faye H. Rodgers[1,a], Julia A. Cai[1], Andre N. Pitaluga[1,b], Dominique Mengin-Lecreulx[2], Mathilde Gendrin[1,3] and George K. Christophides[1]*

[1] Department of Life Sciences, Imperial College London, Exhibition Road, London SW7 2AZ, UK.

[2] Institute for Integrative Biology of the Cell (I2BC), CEA, CNRS, Univ Paris-Sud and Université Paris-Saclay, 91198, Gif-sur-Yvette, France

[3] Institut Pasteur de la Guyane, BP6010 Cayenne, French Guiana, France & Department of Parasites and Insect Vectors, Institut Pasteur, Paris, France

*Corresponding author: g.christophides@imperial.ac.uk

Footnotes

Abstract

Peptidoglycan recognition proteins (PGRPs) constitute the primary means of bacterial recognition in insects. Recent work in the model organism *Drosophila* has revealed the mechanisms by which the complement of PGRPs refine the sensitivity of different tissues to bacterial elicitors, permitting the persistence of commensal bacteria in the gut whilst maintaining vigilance against bacterial infection. Here, we use *in vivo* knockdowns and *in vitro* pull-down assays to investigate the role of the three major isoforms of the transmembrane receptor of the Imd pathway, PGRPLC, in basal immunity in the *Anopheles coluzzii* mosquito midgut. Our results indicate that the mosquito midgut is regionalized in its expression of immune effectors and of PGRPLC1. We show that PGRPLC1 and PGRPLC3 are pulled down with polymeric DAP-type peptidoglycan, while PGRPLC2 and PGRPLC3 co-precipitate in the presence of TCT, a peptidoglycan monomer. These data suggest that, as found in *Drosophila*, discrimination of polymeric and monomeric PGN by *Anopheles* PGRPLC participates in the regulation of the Imd pathway.

Introduction

In insects, bacteria are mainly perceived by the detection of the bacterial cell wall component peptidoglycan (Leulier et al. 2003). Upon recognition, the Imd pathway is one of the major means of signal transduction to initiate antibacterial responses. *Drosophila* Imd pathway activation is tightly regulated in a tissue specific manner, with the gut epithelium being adapted to tolerate the presence of the microbiota. This is achieved through several mechanisms including regulation of ligand availability (Paredes et al. 2011; Zaidman-Remy et al. 2006; Costechareyre et al. 2016), regulation of receptor signaling capacity (Basbous et al. 2011; Maillet et al. 2008; Aggarwal et al. 2008; Kleino et al. 2008; Neyen et al. 2016) and regulation of effector gene transcription (Ryu et al. 2008).

39 *Drosophila* also employs different peptidoglycan recognition proteins (PGRPs) in different tissues as
40 immune receptors or regulators. A diversity of PGRP receptors allows discrimination of the type, the
41 polymerisation status and the level of peptidoglycan that is able to stimulate antimicrobial gene
42 expression (Bosco-Drayon et al. 2012; Neyen et al. 2012). Transmembrane PGRP-LC (FBgn0035976)
43 encodes six isoforms resulting from a combination of 3 splice variants in the extracellular domains
44 (PGRP-LCx, PGRP-LCa and PGRP-LCy) and 2 splice variants in the intracellular domain (Neyen et
45 al. 2016). PGRP-LCx binds both polymeric and monomeric peptidoglycan whilst PGRP-LCa has no
46 peptidoglycan binding capacity (Chang et al. 2005; Mellroth et al. 2005). The pathway can be
47 stimulated by either polymeric peptidoglycan inducing PGRP-LCx-LCx homodimerization or by TCT
48 (tracheal cytotoxin, a peptidoglycan monomer released by growing bacteria) inducing PGRP-LCx-LCa
49 heterodimerization (Chang et al. 2005; Chang et al. 2006; Kaneko et al. 2004; Neyen et al. 2012).
50 PGRP-LCx is shown to be necessary and sufficient for resistance to systemic infection by Gram-
51 negative bacteria, indicating that polymeric peptidoglycan is the primary immune elicitor in the
52 haemolymph, with PGRP-LCa-dependent TCT-induced dimers amplifying the strength of the response
53 (Neyen et al. 2012). The function of PGRP-LCy is less well established (Kaneko et al. 2004; Werner et
54 al. 2003), but could be related to recognition of other types of pathogen-associated molecular patterns
55 (PAMPs) such as the microbial metabolite acetate (Kamareddine et al. 2018). The intracellular splicing
56 variant including exon 4 encodes Imd signaling-inducing PGRP-LC, while the variant including exon 5
57 encodes regulatory PGRP-LC (rPGRP-LC), which sends PGRP-LC to degradation upon specific
58 sensing of polymeric peptidoglycan (Neyen et al. 2016). This downregulation of the Imd pathway via
59 receptor degradation is considered as a way to resolve Imd activation while polymeric peptidoglycan
60 released by lysed bacteria is still present in the haemolymph.

61 A second Imd pathway receptor, PGRP-LE (FBgn0030695), is localized intracellularly where it binds
62 TCT, inducing receptor oligomerization and Imd pathway activation (Kaneko et al. 2006; Lim et al.
63 2006). PGRP-LE is strongly enriched in the *Drosophila* midgut (excluding the cardia) where it is
64 thought to play a significant role in detecting live bacteria and TCT (Bosco-Drayon et al. 2012; Neyen
65 et al. 2012). This PGRP compartmentalization reflects a fine-tuning of the responsiveness of different
66 tissues to their different levels of bacterial exposure. The haemolymph, being a nominally sterile
67 environment, uses extracellular receptors to be highly responsive to both polymeric peptidoglycan and
68 TCT. The posterior midgut, meanwhile, relies largely on an intracellular TCT receptor; here, the Imd
69 pathway is stimulated only when bacterial growth reaches such a threshold that TCT is transported
70 intracellularly. This is appropriate for a tissue that is in constant contact with microbiota.

71 *Anopheles* mosquitoes also rely on the Imd pathway for their response to bacterial infection and for
72 controlling microbiota load, which increases significantly following blood feeding (Meister et al. 2009;
73 Dong, Manfredini, and Dimopoulos 2009). *A. gambiae PGRPLC* (AGAP005203) has a similar genetic
74 architecture to its *Drosophila* orthologue, encoding three main isoforms (PGRPLC1, PGRPLC2 and
75 PGRPLC3) that vary in their extracellular PGRP domains. These PGRP domains have derived from
76 independent duplications between the mosquito and fruit fly lineages, which have been therefore
77 assumed to acquire different functions (Christophides et al. 2002). It has been reported that all
78 mosquito isoforms contribute to resistance to systemic Gram-negative infection, whilst PGRPLC1 and
79 PGRPLC3 only are necessary for resistance to Gram-positive infection (Meister et al. 2009).
80 Additionally, in two mosquito derived cell lines it is found that PGRPLC1 is the only isoform that is
81 necessary for induction of the antimicrobial peptide (AMP) *CEC1* following bacterial challenge (Lin et
82 al. 2007). Overexpression of PGRPLC1 is found to be sufficient for *CEC1* induction even in the
83 absence of bacterial challenge, with PGRPLC3 overexpression having a similar but milder effect (Lin
84 et al. 2007). A non-peptidoglycan-binding PGRP, PGRPLA, is also known to be a positive regulator of
85 the pathway in the gut (Gendrin et al. 2017). Notably, *A. gambiae* does not have a PGRP-LE
86 orthologue. A model has not so far emerged regarding the functions of the different PGRPLC
87 ectodomains in the *A. gambiae* immune response.

88 Given the emerging picture in *Drosophila* of receptor compartmentalization, and the fact that the *A.*
89 *gambiae* genome is lacking in several of the characterized regulators in *Drosophila,* we investigated

90   the role of PGRPLC in basal immune induction in the mosquito gut. We show that the midgut of *A.*
91   *coluzzii* (called *A. gambiae* M molecular form in earlier studies of PGRPLC) is compartmentalized in its
92   expression of the immune effector-encoding transcripts *GAM1*, *CEC1* and *LYSC1,* and of one of the
93   PGRPLC isoforms, *PGRPLC1*. Using isoform specific knockdown, we show that PGRPLC2 and
94   PGRPLC3 both positively regulate REL2-responsive AMPs in the midgut. Functional analyses of
95   recombinant PGRPLC domains indicate that PGRPLC1 and PGRPLC3 are pulled down with
96   polymeric DAP-type peptidoglycan, whilst in the presence of TCT PGRPLC2 and PGRPLC3 co-
97   precipitate.

Materials and Methods

98

Mosquito rearing, blood feeding and antibiotic treatment

99

100   The *A. coluzzii* N'gousso colony was maintained at 27 °C (±1°C), 70-80 % humidity with a 12 h
101   light/dark cycle. All adults were allowed *ad libitum* access to 5 % w/v fructose solution and females
102   were maintained on human blood. 2-3 day old female mosquitoes were used in all experiments,
103   having been exposed to only fructose solution ('sugar-fed'), or 24 h after taking a human blood meal
104   ('blood-fed'). In antibiotic treatments, the blood meal and sugar solutions were supplemented with 60
105   U/ml penicillin, 60 µg/ml streptomycin and 50 µg/ml gentamicin. Antibiotic treatment efficacy was
106   confirmed by qRT-PCR against 16S rRNA.

Gene expression and microbiota analysis

107

108   qRT-PCR was used to assess expression levels of AMPs (*CEC1*, *GAM1* and *LYSC1*), *PGRPLC*
109   transcripts and 16S rRNA load. Midgut tissues were dissected into subregions using a thin needle. For
110   posterior tissue sections, either the whole posterior region (referred to as "posterior") was sampled, or
111   each half of the posterior region (referred to as "proximal posterior" and "distal posterior") was
112   sampled separately, as indicated. Tissues were flash frozen on dry ice and homogenized in TRIzol
113   (Invitrogen) using a Precellys 24 homogenizer (Bertin) with 0.5-mm-wide glass beads (Bertin) or with a
114   pestle-based motorized homogenizer. RNA was extracted according to the TRIzol (Invitrogen)
115   manufacturer's instructions and resuspended in molecular-biology grade, RNase-free water. cDNA
116   was synthesized using PrimeScript Reverse Transcriptase (Takara) or SuperScript III Reverse
117   Transcriptase (ThermoFisher Scientific). qRT-PCR was performed on a 7500 Fast Real Time PCR
118   machine (Applied Biosystems) using a SYBR premix ex Taq kit (Takara). The ribosomal transcript *S7*
119   (AGAP010592) was used as normalization control. qRT-PCR primer sequences are listed in Table S1,
120   and PGRPLC isoform-specific amplicons are represented Fig S1A.

Double stranded RNA preparation and gene knockdown

121

122   Double stranded RNA (dsRNA) was used for transient *in vivo* knockdown of target genes by RNAi.
123   The target region was amplified from total cDNA using primers flanked with the T7 RNA polymerase
124   promoter sequence (primer sequences listed in Table S1) with Phusion Taq polymerase (NEB). PCR
125   products were purified using the QIAquick PCR purification kit (Qiagen). dsRNA was then synthesized
126   from the PCR product by overnight incubation at 37 °C with T7 polymerase and dNTPs from the
127   MEGAscript RNAi kit (ThermoFisher Scientific). dsRNA was purified using the RNeasy kit (Qiagen)
128   and adjusted to a concentration of 6000 ng/µl. 69 nl of 6000 ng/µl dsRNA (totalling 414 µg) was
129   injected into the thorax of CO_2-anaesthetised 0-2-day old female mosquitoes using the Nanoject II
130   (Drummond Scientific). dsRNA against a region of the bacterial *lac* operon (dsLACZ) was injected as a
131   control.

PGRP ectodomain cloning for recombinant protein production

PGRP ectodomains were amplified from an *A. coluzzii* cDNA library by PCR with Phusion polymerase (NEB). The amplified products of the appropriate size were gel extracted using the QIAquick gel extraction kit (Qiagen), cloned by ligation independent cloning using the Ek/LIC cloning kit (Novagen) into the pIEX-10 vector (Novagen) for insect cell expression and verified by sequencing. pIEX-10 introduces an N-terminal strep tag II, a C-terminal His-tag and a secretion signal peptide.

Transfection and stable cell line generation

Sf9 lepidopteran cells were maintained at 27 °C in adherent culture in SF900 II serum free medium. Three stable cell lines were generated, expressing PGRPLC1, PGRPLC2 and PGRPLC3 ectodomains respectively. For transfection, cells were seeded at 80 % confluency in 2.5 ml SF900 II medium. 2 µg pIEX-10+insert and 0.2 µg PIE1- neo (Novagen) were added dropwise with 8 µg Cellfectin II reagent (Invitrogen). PIE1-neo expresses the *neo* gene, facilitating selection in the presence of the antibiotic G418. 24 h post transfection, the medium was replaced with complete medium (SF900 II plus 10 % fetal calf serum (FCS)) and cells were re-plated in serial dilution. After 36 h, the medium was changed to complete medium plus 1 mg/ml G418. This selective medium was refreshed every 4 days for approximately 2 weeks, or until resistant colonies were observed. Selection was reduced to 0.3 mg/ml G418 in complete medium and this concentration was maintained throughout. Once the selected cells reached confluency, a sample of conditioned medium was analyzed by Western blot for expression of recombinant protein.

Recombinant protein purification

Recombinant proteins were purified from conditioned medium by His-tag affinity. TALON beads (Takara; approx. 250 µl per 150 ml conditioned medium) were equilibrated with two washes in 10 volumes of equilibration buffer (50 mM NaH_2PO_4, 300 mM NaCl, pH 7.0). The beads were incubated with conditioned medium, rotating at room temperature, for 2 h. Beads were then washed twice with 20 volumes of wash buffer (50 mM NaH_2PO_4, 300 mM NaCl, 10 mM imidazole, pH 7.0) for 15 min followed by one wash with 5 volumes of wash buffer for 5 min, both at room temperature. His-tagged proteins were eluted in elution buffer (50 mM NaH_2PO_4, 300 mM NaCl, 150 mM imidazole, pH 7.0). Purified proteins were then dialyzed (Amicon Ultra 4 ml dialyzer, 10 kDa pore size) overnight at 4 °C into wash buffer to remove the imidazole for further processing. Where specified, the C-terminal His-tag was cleaved with ProTEV plus protease (Promega), using the TEV cleavage site that was introduced with the reverse primers during cloning. Approximately 200 µg recombinant protein was incubated with ProTEV cleavage buffer, 1 mM DTT and 100 units of ProTEV protease for 3 h at 30 °C. Cleaved protein was isolated from the His tag and the protease itself, which also has a His-tag, using TALON beads as described above (retaining the flow through).

Peptide:N-glycosidase (PNGase F) treatment

5 µg recombinant protein was incubated in denaturation buffer (0.02 % SDS, 10 mM β-mercaptoethanol) at 100 °C for 10 min before being incubated with 2.5 units PNGase F and 0.8 % Triton X-100 at 37 °C for 3 h.

Western blotting

After separation by SDS-PAGE, proteins were transferred to a nitrocellulose membrane by semi dry transfer (15 V for 30 min) and membranes blocked in phosphate buffered saline plus 1 % Tween-20 (PBST) with 3 % bovine serum albumin (BSA), either overnight at 4 °C or for 1 h at room temperature. Primary antibody was added in fresh blocking buffer at the specified concentration and incubated overnight at 4 °C. After three 10 min washes in PBST, blots were incubated with the specified secondary antibody conjugated with horseradish peroxidase (HRP) at a 1:10000 dilution in PBST with

177 3 % BSA for 1 h at room temperature, before three further washes in PBST. Blots were exposed with
178 ECL chemiluminescence substrate (Pierce) and visualized with a Biorad Chemidoc Imager.

Peptidoglycan preparation

180 DAP-type peptidoglycan polymer was purified from the *E. coli* BW25113 Δ*lpp*::Cm^R strain that does
181 not express the Lpp lipoprotein, as described (Leulier et al. 2003). The GlcNAc-MurNAc(anhydro)-L-
182 Ala-D-iGlu-*meso*-DAP-D-Ala peptidoglycan monomer fragment (designated as TCT, tracheal
183 cytotoxin) was obtained by peptidoglycan digestion with SltY transglycosylase and purified by HPLC
184 as previously described (Stenbak et al. 2004).

Peptidoglycan co-precipitation assay

186 Recombinant protein (100 µg/ml) was incubated with insoluble peptidoglycan from *Escherichia coli* (1
187 mg/ml) in 50 µl binding buffer (150 mM NaCl, 20 mM HEPES, pH 7.5) for 1 h at room temperature,
188 rotating. The insoluble peptidoglycan was then pelleted by centrifugation (13000 g, 5 min). The pellet
189 was washed three times in 1 ml binding buffer and resuspended in 50 µl binding buffer. Pellet and
190 supernatant fractions were analyzed by Western blot, using a primary antibody against the N-terminal
191 strep tag II.

PGRPLC co-precipitation assay

193 For protein-protein co-precipitation assays, recombinant protein after cleavage of the His-tag (100
194 µg/ml) was incubated with recombinant protein that retained its His-tag (100 µg/ml) in the presence of
195 an approximately 5-fold molar excess of TCT (20 µM) in 50 µl binding buffer for 1 h at room
196 temperature, rotating. His-tagged protein and any interacting protein were then purified by His-tag
197 affinity. The flow through and bead bound fractions were analyzed for their protein content by Western
198 blot, probing for the N-terminal strep tag II.

Statistical analysis

200 qRT-PCR expression data (including 16S analysis) were analyzed with linear mixed effect regression
201 models using the lme4 package in R (version 3.1.2). Mosquito batch (i.e., experimental replicate) was
202 included as a random effect, with tissue section and/or dsRNA as fixed effects. When examining the
203 effect of dsRNA in different tissues, a tissue:dsRNA interaction term was fitted first (together with the
204 main effect terms). If this significantly improved the fit of the model (as assessed by ANOVA), we go
205 on to report the effect of dsRNA in each tissue independently (expression ~ dsRNA + (1|replicate)).
206 Otherwise, the reported p value is the result of an ANOVA test after removing dsRNA from the full
207 model (expression ~ tissue + dsRNA + (1|replicate)).

Results

**AMP expression and *PGRPLC1* expression are spatially heterogeneous along the mosquito
midgut**

211 We examined whether the *A. coluzzii* gut tissue is spatially heterogeneous in its immune activity, and
212 how this putative heterogeneity might be related to the presence of the gut microbiota. Midguts were
213 micro-dissected into three main regions: the cardia, anterior and posterior (Fig 1A). The abundance of
214 bacterial 16S rRNA and the expression of transcripts of the microbiota-dependent antimicrobial
215 peptides (AMPs; Rodgers et al. 2017) *CEC1* (AGAP000693)*, GAM1* (AGAP008645) and *LYSC1*
216 (AGAP007347) were analyzed by qRT-PCR. We observed that bacterial proliferation upon blood
217 feeding is limited to the posterior section of the gut, the region which harbours the blood bolus (Fig
218 1B). Strikingly, all three AMPs analyzed were heterogeneously expressed across the length of both

219 sugar-fed and blood-fed guts, with expression being higher in the cardia and anterior regions than the
220 posterior (Fig 1C-E), despite the abundance of the microbiota in this region after blood feeding. We
221 assessed whether all regions of the gut are able to respond transcriptionally to the microbiota by
222 comparing AMP expression in control mosquitoes with mosquitoes that have been treated with a
223 robust cocktail of antibiotics (Fig 1C-E). Expression of one AMP (*GAM1* in the sugar-fed posterior
224 region) or all three AMPs (in all other regions) was lower after antibiotic treatment; thus, we conclude
225 that the whole length of the gut epithelium is able to respond to microbiota-derived bacterial elicitors.

226 We next analyzed the expression pattern of the three major PGRPLC isoforms. We found that the
227 expression of *PGRPLC1* correlates well with that of the AMPs analyzed, being more highly expressed
228 in the cardia and anterior regions than in the posterior (Fig 1F). *PGRPLC2* and *PGRPLC3* do not vary
229 in their expression across the length of the gut (Fig S1). Altogether, these data show that the
230 expression of *CEC1, GAM1, LYSC1 and PGRPLC1* vary significantly along the length of the gut,
231 though their expression pattern appears to be uncoupled from levels of exposure to commensal
232 bacteria in the different regions.

PGRPLC2 and PGRPLC3 are positive regulators of REL2-responsive AMPs in the midgut

234 Given that PGRPLC-dependent activation of the Imd pathway plays a role in controlling the mosquito
235 gut microbiota (Dong, Manfredini, and Dimopoulos 2009; Meister et al. 2009), we next sought to
236 decipher which PGRPLC isoforms are responsible for stimulating Imd activity in the midgut.

237 We first determined which AMPs are transcriptionally responsive to the Imd pathway in the sugar-fed
238 and blood-fed gut by monitoring the expression of *GAM1, LYSC1* and *CEC1* after injection of dsRNA
239 against the Imd pathway transcription factor REL2 (AGAP006747) (Fig 2, Fig S2, Fig S3). Of the
240 AMPs analyzed, we found *GAM1* expression to be responsive to *REL2* knockdown across the sugar-
241 fed gut ($p<0.05$, Fig 2A). *REL2* knockdown had no significant effect on *CEC1* or *LYSC1* expression in
242 the sugar-fed gut (Fig S3A-B).

243 We next injected dsRNA against each specific PGRPLC ectodomain, trying to recapitulate the effect
244 on *GAM1* expression (Fig 2A). As observed previously (Meister et al. 2009), we achieved limited and
245 variable knockdown efficiency against individual PGRPLC isoforms (Fig S2). Nevertheless, we found
246 that *PGRPLC2* dsRNA caused a significant reduction in *GAM1* expression in the cardia ($p<0.05$) and
247 anterior ($p<0.05$) regions of the sugar-fed midgut. *PGRPLC3* dsRNA had no effect in any region of the
248 sugar-fed midgut. *PGRPLC1* dsRNA resulted in a significant increase in *GAM1* expression in the
249 anterior region ($p<0.05$), but interestingly not in the cardia despite this region having very high
250 *PGRPLC1* expression.

251 After blood feeding, *GAM1* remained responsive to REL2 throughout the gut ($p<0.05$, Fig S3C),
252 though no PGRPLC isoforms had any effect on *GAM1* expression. We also observed a significant
253 reduction in *LYSC1* expression upon REL2 knockdown in the cardia ($p=0.05$) and anterior ($p<0.05$)
254 regions, with the posterior region showing the same trend (Fig 2B). Concurrently, we found PGRPLC2
255 dsRNA to cause a reduction in *LYSC1* expression in the posterior region ($p<0.05$) and PGRPLC3
256 dsRNA to cause a reduction in *LYSC1* expression in the cardia ($p<0.05$) and posterior ($p<0.01$)
257 regions.

258 Altogether, these data confirm that the AMPs *GAM1, CEC1* and *LYSC1* are REL2-responsive in at
259 least some regions of the midgut. PGRPLC2 and PGRPLC3 also both act as positive regulators of two
260 of these AMPs. Despite PGRPLC1 being known to be able to induce the Imd pathway (Lin et al.
261 2007), we did not find evidence for this isoform acting as a positive Imd regulator in the midgut. Our
262 data rather suggests that PGRPLC1 could be acting as a negative regulator, though we cannot rule
263 out that PGRPLC1-dependent signaling to other pathways induces dysbiosis, causing the observed
264 induction of *GAM1* expression.

6

PGRPLC1 and PGRPLC3 co-precipitate with polymeric DAP-type peptidoglycan

In order to understand further the differing functions of the PGRPLC isoforms, their PGRP domains were recombinantly produced and subjected to *in vitro* functional analysis. The recombinant PGRP domains of the three major isoforms were secreted from Sf9 lepidopteran cells and purified from conditioned media with a C-terminal His-tag (Fig S4A). The His-tags were cleaved before further functional analysis to avoid artefactual interaction between them and peptidoglycan (Basbous et al. 2011; Persson, Oldenvi, and Steiner 2007). PGRPLC1 and PGRPLC3 were observed to migrate as a double and triple band, respectively, whilst PGRPLC2 migrates as a single band (Fig S4B). We hypothesized that this may be due to glycosylation, a common posttranslational modification in secreted and membrane bound proteins. All of the ectodomains have predicted O-glycosylation sites, whilst PGRPLC1 and PGRPLC3 additionally have two and three predicted N-glycosylation sites, respectively (Fig S4C). Treatment with PNGase F, an N-glycosidase, indeed resulted in a shift in the migration of PGRPLC1 and PGRPLC3 with no effect on PGRPLC2 (Fig S4D), suggesting that PGRPLC1 and PGRPLC3 undergo N-glycosylation.

We first looked at the ability of the three PGRPLC ectodomains to interact with peptidoglycan. As the vast majority of bacteria present in the gut microbiota are Gram-negative, we used DAP-type peptidoglycan purified from *E. coli* for this purpose. Each PGRPLC isoform was incubated with insoluble peptidoglycan, and the supernatant and washed pellet analyzed by Western blot. Under the conditions used, PGRPLC1 and PGRPLC3 were both pulled down with the polymeric peptidoglycan, whilst PGRPLC2 remained in the supernatant fraction (Fig 3A). When isoforms were combined pairwise and co-precipitated with peptidoglycan, we observed a protein migrating as a single band (likely PGRPLC2) in the supernatant fraction of both the PGRPLC1/PGRPLC2 and PGRPLC2/PGRPLC3 combinations (Fig 3B). Whilst we cannot rule out some level of PGRPLC2-peptidoglycan interaction, we conclude that PGRPLC1 and PGRPLC3 co-precipitate with polymeric DAP-type peptidoglycan, both alone and in the presence of other PGRPLC isoforms.

PGRPLC2 and PGRPLC3 co-precipitate in the presence of TCT

Next, we considered which of the PGRP domains could interact with one another in the presence of the peptidoglycan monomer, TCT. To do this, we combined one isoform with its His-tag with another isoform whose His-tag had been cleaved off, in the presence of TCT. Purifying by His-tag affinity, we then pulled down the His-tagged protein and observed whether the other, non-His tagged, isoform pulled down with it or remained in the flow-through fraction (Fig 4A). When probing initially with anti-strep tag II, we found that the PGRPLC2/PGRPLC3 combination led to near complete pull down (Fig 4A), with no free PGRPLC3 being observed in the flow-through fraction. This was not due to residual His-tag being retained on PGRPLC3, as in combination with both PGRPLC3(His) and PGRPLC1(His) a large proportion of PGRPLC3 is found in the flow-through fraction. To validate this finding, we performed the reciprocal experiment, pulling down PGRPLC1 and PGRPLC2 with PGRPLC3(His) (Fig 4B). As expected, PGRPLC2 appears almost entirely in the bound fraction whilst PGRPLC1 appears mostly in the free fraction, again with a small proportion in the bound fraction. In addition to the PGRPLC2/LC3 interaction, we also observed the appearance of bands at sizes that correspond to dimers and higher oligomers (Fig 4). These bands were present largely in the bound fractions, i.e., in the presence of the His-tag. We cannot therefore rule out these dimers being an artefact caused by the presence of the His-tag, a proposition that has some precedence (Wu and Filutowicz 1999). Nevertheless, we conclude that, in the presence of TCT, PGRPLC2 and PGRPLC3 show specific co-precipitation with one another.

Discussion

We demonstrate here that the mosquito midgut is heterogeneous in its expression of immune effectors and at least one immune receptor. In particular, we observe higher expression of the AMPs *GAM1*, *CEC1* and *LYSC1* in the cardia region compared with the posterior region of sugar-fed and blood-fed

midguts. The *Drosophila* midgut is already understood to be compartmentalized in its immune and digestive function (Buchon and Osman 2015), with enrichment of Imd dependent immune genes in the cardia region (Buchon et al. 2013; Tzou et al. 2000). This likely both ensures that exogenous bacteria entering the gut encounter a robust initial immune response and allows the microbiota in the posterior region to persist. A question arising from this finding is the mechanism by which the gut epithelium mediates this heterogeneity, given that it is exposed to, and indeed responds to, bacterial ligand along its length. Despite observing a very similar spatial heterogeneity in the expression of PGRPLC1, we were not able to detect any clear isoform-specific functionality in this region, perhaps suggesting that PGRPLC receptor variation does not underlie this basal variation in immunogenicity.

Previous structural modelling predicted that dimerization of all isoform-isoform combinations was feasible, except for PGRPLC3 homodimers (Meister et al. 2009). To our knowledge, the experiments presented here are the first to explore *in vitro* the functionality of the mosquito PGRPLC isoforms. Our results show that PGRPLC1 and PGRPLC3 co-precipitate with polymeric DAP-type peptidoglycan. In the presence of TCT, PGRPLC2 and PGRPLC3 co-precipitate with one another. These data are consistent with a model whereby PGRPLC2 plays a similar role to *Drosophila* PGRP-LCa, which acts as an adaptor to PGRP-LCx in the presence of TCT, while PGRPLC3 is a PGRP-LCx equivalent.

This model is supported by previously published data on the functionality of the PGRPLC isoforms. All isoforms contribute to resistance to systemic Gram-negative infection, whilst only PGRPLC1 and PGRPLC3 are necessary for resistance to Gram-positive infection (Meister et al. 2009). Given that only Gram-negative bacteria shed TCT, this is consistent with PGRPLC2 only playing a role in the presence of Gram-negatives. In *A. gambiae* cultured cells, overexpression of either PGRPLC1 or PGRPLC3, but not PGRPLC2, is sufficient to induce *CEC1* expression in the absence of infection (Lin et al. 2007). Again, this is consistent with PGRPLC2 acting as an adapter and alone being unable to dimerize with itself.

In the knockdown experiments presented here, we find both PGRPLC2 and PGRPLC3 acting as positive regulators of REL2 responsive AMPs. We also observed *GAM1* to be responsive to REL2 after blood feeding, but did not observe knockdown of any single PGRPLC isoform to reproduce this effect. This could suggest that there is redundancy amongst the three PGRPLC isoforms under these conditions, or indeed that PGRPLC is able to dimerize with other partners to stimulate the pathway, such as PGRPLA (Gendrin et al. 2017). This model is also consistent with our observation that PGRPLC3 is not necessary for AMP induction in the sugar-fed gut, suggesting that PGRPLC2 can dimerize with another partner under these conditions.

Interestingly, PGRPLC1 silencing was found to lead to stimulation of the Imd pathway in the anterior part of the midgut. This is intriguing, considering that the same isoform is known to be able to induce the Imd pathway (Lin et al. 2007). However, it has been shown in the *Drosophila* gut that a single peptidoglycan receptor, PGRP-LE, induces the Imd pathway in response to infectious bacteria, while promoting tolerance to the microbiota via induction of Imd negative regulators (Bosco-Drayon et al. 2012). *Drosophila* PGRP-LC also has a dual role in Imd induction and negative regulation, depending on its intracellular domain (Neyen et al. 2016).

Together, our data indicate that *Anopheles* PGRPLC isoforms can discriminate polymeric and monomeric peptidoglycan. They also suggest that PGRPLC2 acts as an adapter to PGRPLC3 for the specific sensing of TCT, leading to the induction of the Imd pathway. Finally, they add a putative regulatory role for PGRPLC1, besides its shown Imd-inducing activity.

Acknowledgements

Figure legends

362 **Figure 1. Spatial heterogeneity of *AMP* and *PGRPLC1* expression in the mosquito gut.**

363 (A) Schematic of the mosquito gut, with dissected midgut regions indicated. (B) 16S rRNA distribution
364 throughout the gut of sugar-fed and blood-fed females, determined by qRT-PCR on cDNA using
365 universal 16S primers. Each point represents a pool of tissues from 15-30 individual mosquitoes,
366 derived from 5 (blood-fed) and up to 8 (sugar-fed) independent batches of mosquito. Bacterial load
367 significantly increases in the posterior region after blood feeding: $p < 0.05$, ANOVA following linear
368 mixed effect regression model fitting. (C-E) Expression of *CEC1*, *GAM1* and *LYSC1* throughout the
369 gut of sugar-fed and blood-fed females, with or without antibiotic feeding. Each point represents a pool
370 of tissues from 15-30 individual mosquitoes, derived from 5 (blood-fed) and up to 6 (sugar-fed)
371 independent batches of mosquito. For all three AMPs, tissue of origin had a statistically significant
372 effect on AMP expression level: *CEC1* $p < 0.001$, *GAM1* $p < 0.001$, *LYSC1* $p < 0.01$, ANOVA following
373 linear mixed effect regression model fitting. (F) Expression of *PGRPLC1* throughout the gut of sugar-
374 fed mosquitoes. Each point represents a pool of tissues, of 15-30 individual mosquitoes per pool,
375 derived from 5 independent batches of mosquito. Tissue of origin had a statistically significant effect
376 on *PGRPLC1* expression level: $p < 0.01$, ANOVA following linear regression model fitting. In graphs B-
377 F, the shapes of the points for the sugar-fed posterior region indicate whether samples were from the
378 whole posterior region (circles), the proximal half (squares) or the distal half (triangles).

379 **Figure 2. The effect of REL2 and PGRPLC isoform knockdown on *GAM1* and *LYSC1* expression**
380 **in the mosquito gut.**

381 (A) *GAM1* expression in different regions of the sugar-fed midgut following injection of dsRNA against
382 LACZ (control), REL2 or specific PGRPLC isoforms. REL2 dsRNA causes a significant reduction in
383 *GAM1* expression independently of tissue of origin ($p < 0.05$), PGRPLC1 dsRNA causes a significant
384 increase in *GAM1* expression in the anterior region ($p < 0.05$), and PGRPLC2 dsRNA causes a
385 significant reduction in *GAM1* expression in the cardia ($p < 0.05$) and anterior regions ($p < 0.05$). The
386 shape of the data points indicate whether the sample represents the whole posterior region (circles),
387 the proximal half (squares) or the distal half (triangles). (B) *LYSC1* expression in different regions of
388 the blood-fed midgut following injection of dsRNA against LACZ (control), REL2 or specific PGRPLC
389 isoforms. REL2 dsRNA causes a significant reduction in *LYSC1* expression in the cardia ($p = 0.05$) and
390 anterior ($p < 0.05$) regions, PGRPLC2 dsRNA causes a significant reduction in *LYSC1* expression
391 specifically in the posterior region ($p < 0.05$), and PGRPLC3 dsRNA causes a significant reduction in
392 *LYSC1* expression in the cardia ($p < 0.05$) and posterior ($p < 0.01$) regions. In both panels, each point
393 represents a pool of tissues from 10-20 individual mosquitoes, derived from 3 (REL2, PGRPLC1 and
394 PGRPLC2) or 4 (PGRPLC3 and LACZ) independent batches of mosquito. P values are derived from
395 ANOVA tests following linear mixed effect regression model fitting.

396 **Figure 3. PGRPLC1 and PGRPLC3 co-precipitate with polymeric DAP-type peptidoglycan.**

397 (A) Pull down assays using insoluble, polymeric DAP-type peptidoglycan and single PGRPLC
398 isoforms. Blot shows one of three independent replicates, each giving the same result. (B) Pull down
399 assays using insoluble, polymeric DAP-type peptidoglycan and combinations of PGRPLC isoforms, as
400 indicated. Blot shows one of two independent replicates, both giving the same result. Western blots
401 are non-reducing and were probed with anti-strep tag II antibody (1:1000 in 3% BSA). In=input
402 (recombinant PGRP that had not been exposed to peptidoglycan); F=free; B=bound.

403 **Figure 4. PGRPLC2 and PGRPLC3 co-precipitate in the presence of TCT.**

404 (A-B) The PGRPLC2 ectodomain interacts with the PGRPLC3 ectodomain in the presence of TCT.
405 His-tagged PGRPLC isoforms were incubated with non-His tagged PGRPLC isoforms, pulled down by

His tag affinity and the free (F) and bound (B) fractions analyzed. Western blots are non-reducing and were probed with anti-strep- tag II antibody (1:1000 in 3% BSA).

Figure S1. Expression of *PGRPLC2* and *PGRPLC3* does not vary along the length of the gut.

(A) Schematic indicating qRT-PCR primer positioning on the *PGRPLC* transcript. (B) Expression of the *PGRPLC2* and *PGRPLC3* transcripts throughout the gut of sugar-fed mosquitoes. Each point represents a pool of tissues, of 15-30 individual mosquitoes per pool, derived from 5 independent batches of mosquito.

Figure S2. Knockdown efficiencies of REL2 and PGRPLC isoforms in different regions of the sugar-fed and blood-fed gut.

Each point represents a pool of tissues, of 10-20 individual mosquitoes per pool, derived from 3 (REL2, PGRPLC1 and PGRPLC2) or 4 (PGRPLC3 and LACZ) independent batches of mosquito. For the sugar-fed posterior region, point shapes indicate whether the sample represents the whole posterior region (circles), the proximal half (squares) or the distal half (triangles). Knockdown was quantified concurrently with AMP expression analysis, 24 h (sugar-fed) or 48 h (blood-fed) after dsRNA injection.

Figure S3. The effect of REL2 and PGRPLC isoform knockdown on *GAM1, CEC1* and *LYSC1* expression in the mosquito gut.

(A) *CEC1* expression in different regions of the sugar-fed midgut following injection of dsRNA against LACZ (control), REL2 or specific PGRPLC isoforms. PGRPLC2 dsRNA causes a significant reduction in *CEC1* expression in the cardia region ($p<0.05$). (B) *LYSC1* expression in different regions of the sugar-fed midgut following injection of dsRNA against LACZ (control), REL2 or specific PGRPLC isoforms. (C) *GAM1* expression in different regions of the blood-fed midgut following injection of dsRNA against LACZ (control), REL2 or specific PGRPLC isoforms. REL2 dsRNA causes a significant reduction in *GAM1* expression independently of tissue of origin ($p<0.05$). (D) *CEC1* expression in different regions of the blood-fed midgut following injection of dsRNA against LACZ (control), REL2 or specific PGRPLC isoforms. (A-D) Each point represents a pool of tissues, of 10-20 individual mosquitoes per pool, derived from 3 (REL2, PGRPLC1 and PGRPLC2) or 4 (PGRPLC3 and LACZ) independent batches of mosquito. p values are the result of ANOVAs following linear mixed effect regression model fitting. For the sugar-fed posterior region, point shapes indicate whether the sample represents the whole posterior region (circles), the proximal half (squares) or the distal half (triangles).

Figure S4. Production of recombinant PGRPLC ectodomains.

(A) Schematic of the expression region in the pIEX-10 vector used for recombinant protein production. (B) Coomassie stained gel of purified proteins before and after His-tag cleavage. (C) Glycosylation sites predicted using the GlycoEP server (Chauhan, Rao, and Raghava 2013) using Binary Profile of Patterns (BPP) prediction with SVM threshold set to 0.0. (D) PNGase F treatment of recombinant PGRPs. Western blot probed with anti His antibody (1:2000 in 3% BSA).

References

Aggarwal, K., F. Rus, C. Vriesema-Magnuson, D. Erturk-Hasdemir, N. Paquette, and N. Silverman. 2008. 'Rudra interrupts receptor signaling complexes to negatively regulate the IMD pathway', *PLoS Pathog*, 4: e1000120.

Basbous, N., F. Coste, P. Leone, R. Vincentelli, J. Royet, C. Kellenberger, and A. Roussel. 2011. 'The Drosophila peptidoglycan-recognition protein LF interacts with peptidoglycan-recognition protein LC to downregulate the Imd pathway', *EMBO Rep*, 12: 327-33.

449 Bosco-Drayon, V., M. Poidevin, I. G. Boneca, K. Narbonne-Reveau, J. Royet, and B. Charroux. 2012.
450   'Peptidoglycan sensing by the receptor PGRP-LE in the Drosophila gut induces immune responses
451   to infectious bacteria and tolerance to microbiota', *Cell Host Microbe*, 12: 153-65.
452 Buchon, N., and D. Osman. 2015. 'All for one and one for all: Regionalization of the Drosophila
453   intestine', *Insect Biochem Mol Biol*, 67: 2-8.
454 Buchon, N., D. Osman, F. P. David, H. Y. Fang, J. P. Boquete, B. Deplancke, and B. Lemaitre. 2013.
455   'Morphological and molecular characterization of adult midgut compartmentalization in Drosophila',
456   *Cell Rep*, 3: 1725-38.
457 Chang, C. I., Y. Chelliah, D. Borek, D. Mengin-Lecreulx, and J. Deisenhofer. 2006. 'Structure of
458   tracheal cytotoxin in complex with a heterodimeric pattern-recognition receptor', *Science*, 311:
459   1761-4.
460 Chang, C. I., K. Ihara, Y. Chelliah, D. Mengin-Lecreulx, S. Wakatsuki, and J. Deisenhofer. 2005.
461   'Structure of the ectodomain of Drosophila peptidoglycan-recognition protein LCa suggests a
462   molecular mechanism for pattern recognition', *Proc Natl Acad Sci U S A*, 102: 10279-84.
463 Chauhan, J. S., A. Rao, and G. P. Raghava. 2013. 'In silico platform for prediction of N-, O- and C-
464   glycosites in eukaryotic protein sequences', *PLoS One*, 8: e67008.
465 Christophides, G. K., E. Zdobnov, C. Barillas-Mury, E. Birney, S. Blandin, C. Blass, P. T. Brey, F. H.
466   Collins, A. Danielli, G. Dimopoulos, C. Hetru, N. T. Hoa, J. A. Hoffmann, S. M. Kanzok, I. Letunic,
467   E. A. Levashina, T. G. Loukeris, G. Lycett, S. Meister, K. Michel, L. F. Moita, H. M. Muller, M. A.
468   Osta, S. M. Paskewitz, J. M. Reichhart, A. Rzhetsky, L. Troxler, K. D. Vernick, D. Vlachou, J. Volz,
469   C. von Mering, J. Xu, L. Zheng, P. Bork, and F. C. Kafatos. 2002. 'Immunity-related genes and
470   gene families in Anopheles gambiae', *Science*, 298: 159-65.
471 Costechareyre, D., F. Capo, A. Fabre, D. Chaduli, C. Kellenberger, A. Roussel, B. Charroux, and J.
472   Royet. 2016. 'Tissue-Specific Regulation of Drosophila NF-x03BA;B Pathway Activation by
473   Peptidoglycan Recognition Protein SC', *J Innate Immun*, 8: 67-80.
474 Dong, Y., F. Manfredini, and G. Dimopoulos. 2009. 'Implication of the mosquito midgut microbiota in
475   the defense against malaria parasites', *PLoS Pathog*, 5: e1000423.
476 Gendrin, M., F. Turlure, F. H. Rodgers, A. Cohuet, I. Morlais, and G. K. Christophides. 2017. 'The
477   Peptidoglycan Recognition Proteins PGRPLA and PGRPLB Regulate Anopheles Immunity to
478   Bacteria and Affect Infection by Plasmodium', *J Innate Immun*, 9: 333-42.
479 Kamareddine, L., W. P. Robins, C. D. Berkey, J. J. Mekalanos, and P. I. Watnick. 2018. 'The
480   Drosophila Immune Deficiency Pathway Modulates Enteroendocrine Function and Host
481   Metabolism', *Cell Metab*, 28: 449-62.e5.
482 Kaneko, T., W. E. Goldman, P. Mellroth, H. Steiner, K. Fukase, S. Kusumoto, W. Harley, A. Fox, D.
483   Golenbock, and N. Silverman. 2004. 'Monomeric and polymeric gram-negative peptidoglycan but
484   not purified LPS stimulate the Drosophila IMD pathway', *Immunity*, 20: 637-49.
485 Kaneko, T., T. Yano, K. Aggarwal, J. H. Lim, K. Ueda, Y. Oshima, C. Peach, D. Erturk-Hasdemir, W.
486   E. Goldman, B. H. Oh, S. Kurata, and N. Silverman. 2006. 'PGRP-LC and PGRP-LE have essential
487   yet distinct functions in the drosophila immune response to monomeric DAP-type peptidoglycan',
488   *Nat Immunol*, 7: 715-23.
489 Kleino, A., H. Myllymaki, J. Kallio, L. M. Vanha-aho, K. Oksanen, J. Ulvila, D. Hultmark, S. Valanne,
490   and M. Ramet. 2008. 'Pirk is a negative regulator of the Drosophila Imd pathway', *J Immunol*, 180:
491   5413-22.
492 Leulier, F., C. Parquet, S. Pili-Floury, J. H. Ryu, M. Caroff, W. J. Lee, D. Mengin-Lecreulx, and B.
493   Lemaitre. 2003. 'The Drosophila immune system detects bacteria through specific peptidoglycan
494   recognition', *Nat Immunol*, 4: 478-84.
495 Lim, J. H., M. S. Kim, H. E. Kim, T. Yano, Y. Oshima, K. Aggarwal, W. E. Goldman, N. Silverman, S.
496   Kurata, and B. H. Oh. 2006. 'Structural basis for preferential recognition of diaminopimelic acid-type
497   peptidoglycan by a subset of peptidoglycan recognition proteins', *J Biol Chem*, 281: 8286-95.
498 Lin, H. U. I., Lingmin Zhang, Coralia Luna, Ngo T. Hoa, and Liangbiao Zheng. 2007. 'A splice variant
499   of PGRP-LC required for expression of antimicrobial peptides in Anopheles gambiae', *Insect
500   Science*, 14: 185-92.

501 Maillet, F., V. Bischoff, C. Vignal, J. Hoffmann, and J. Royet. 2008. 'The Drosophila peptidoglycan
502   recognition protein PGRP-LF blocks PGRP-LC and IMD/JNK pathway activation', *Cell Host*
503   *Microbe*, 3: 293-303.
504 Meister, S., B. Agianian, F. Turlure, A. Relogio, I. Morlais, F. C. Kafatos, and G. K. Christophides.
505   2009. 'Anopheles gambiae PGRPLC-mediated defense against bacteria modulates infections with
506   malaria parasites', *PLoS Pathog*, 5: e1000542.
507 Mellroth, P., J. Karlsson, J. Hakansson, N. Schultz, W. E. Goldman, and H. Steiner. 2005. 'Ligand-
508   induced dimerization of Drosophila peptidoglycan recognition proteins in vitro', *Proc Natl Acad Sci*
509   *U S A*, 102: 6455-60.
510 Neyen, C., M. Poidevin, A. Roussel, and B. Lemaitre. 2012. 'Tissue- and ligand-specific sensing of
511   gram-negative infection in drosophila by PGRP-LC isoforms and PGRP-LE', *J Immunol*, 189: 1886-
512   97.
513 Neyen, C., C. Runchel, F. Schupfer, P. Meier, and B. Lemaitre. 2016. 'The regulatory isoform rPGRP-
514   LC induces immune resolution via endosomal degradation of receptors', *Nat Immunol*, 17: 1150-8.
515 Paredes, J. C., D. P. Welchman, M. Poidevin, and B. Lemaitre. 2011. 'Negative regulation by amidase
516   PGRPs shapes the Drosophila antibacterial response and protects the fly from innocuous infection',
517   *Immunity*, 35: 770-9.
518 Persson, C., S. Oldenvi, and H. Steiner. 2007. 'Peptidoglycan recognition protein LF: a negative
519   regulator of Drosophila immunity', *Insect Biochem Mol Biol*, 37: 1309-16.
520 Ryu, J. H., S. H. Kim, H. Y. Lee, J. Y. Bai, Y. D. Nam, J. W. Bae, D. G. Lee, S. C. Shin, E. M. Ha, and
521   W. J. Lee. 2008. 'Innate immune homeostasis by the homeobox gene caudal and commensal-gut
522   mutualism in Drosophila', *Science*, 319: 777-82.
523 Stenbak, C. R., J. H. Ryu, F. Leulier, S. Pili-Floury, C. Parquet, M. Hervé, C. Chaput, I. G. Boneca, W.
524   J. Lee, B. Lemaitre, and D. Mengin-Lecreulx. 2004. 'Peptidoglycan molecular requirements allowing
525   detection by the Drosophila immune deficiency pathway', *J Immunol*, 173: 7339-48.
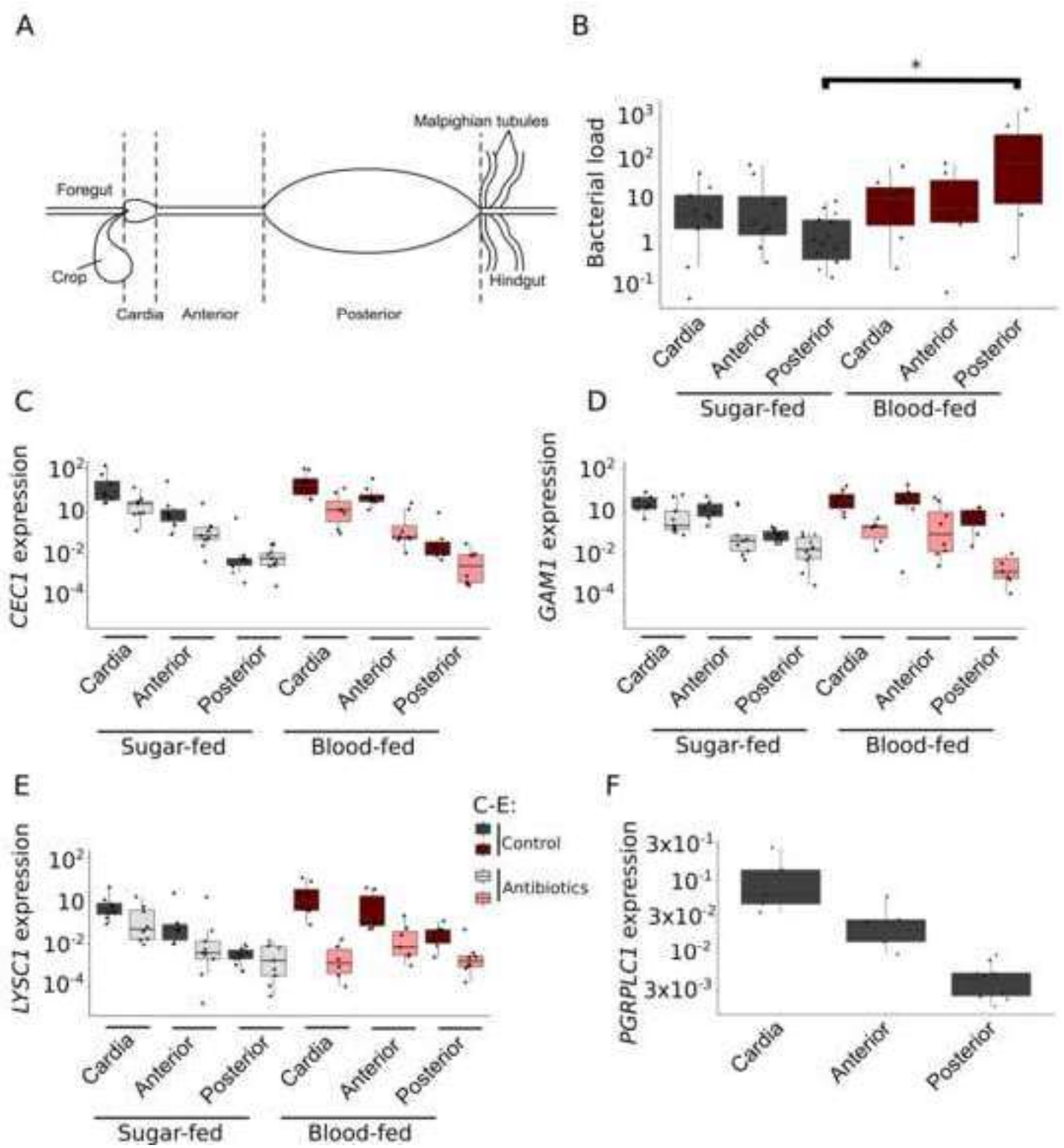526 Tzou, P., S. Ohresser, D. Ferrandon, M. Capovilla, J. M. Reichhart, B. Lemaitre, J. A. Hoffmann, and
527   J. L. Imler. 2000. 'Tissue-specific inducible expression of antimicrobial peptide genes in Drosophila
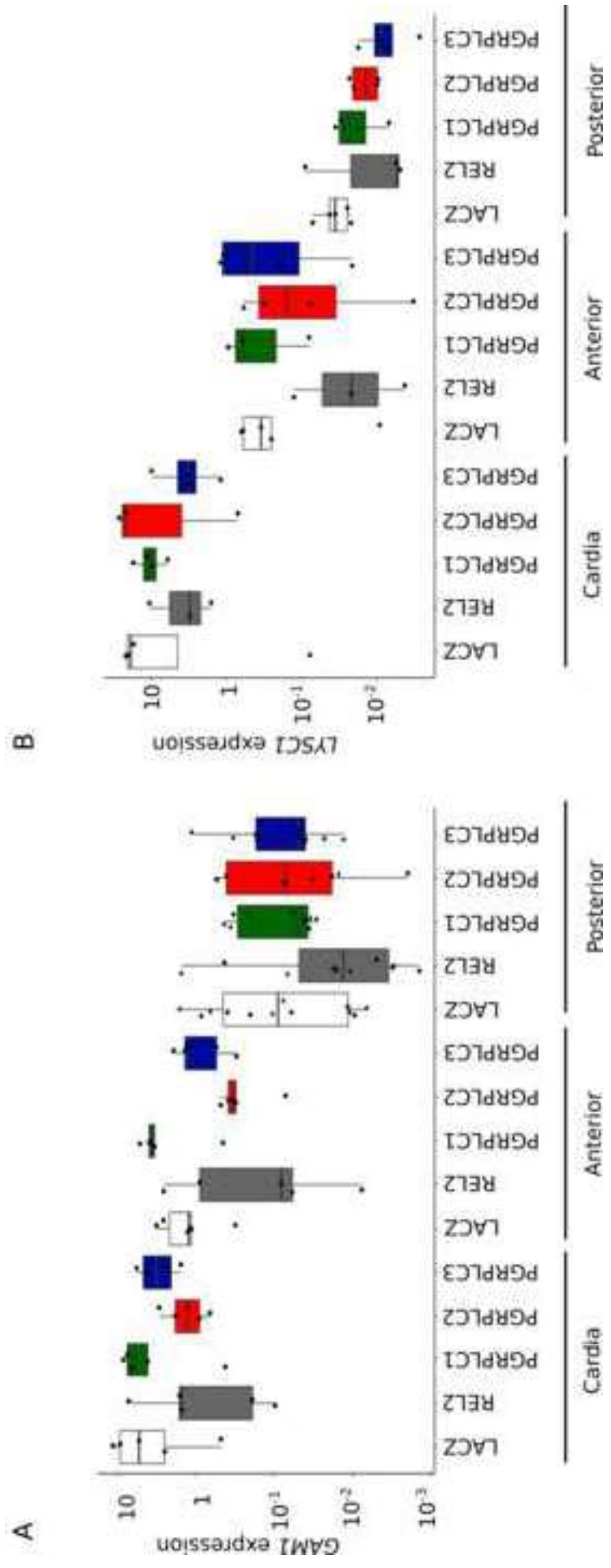528   surface epithelia', *Immunity*, 13: 737-48.
529 Werner, T., K. Borge-Renberg, P. Mellroth, H. Steiner, and D. Hultmark. 2003. 'Functional diversity of
530   the Drosophila PGRP-LC gene cluster in the response to lipopolysaccharide and peptidoglycan', *J*
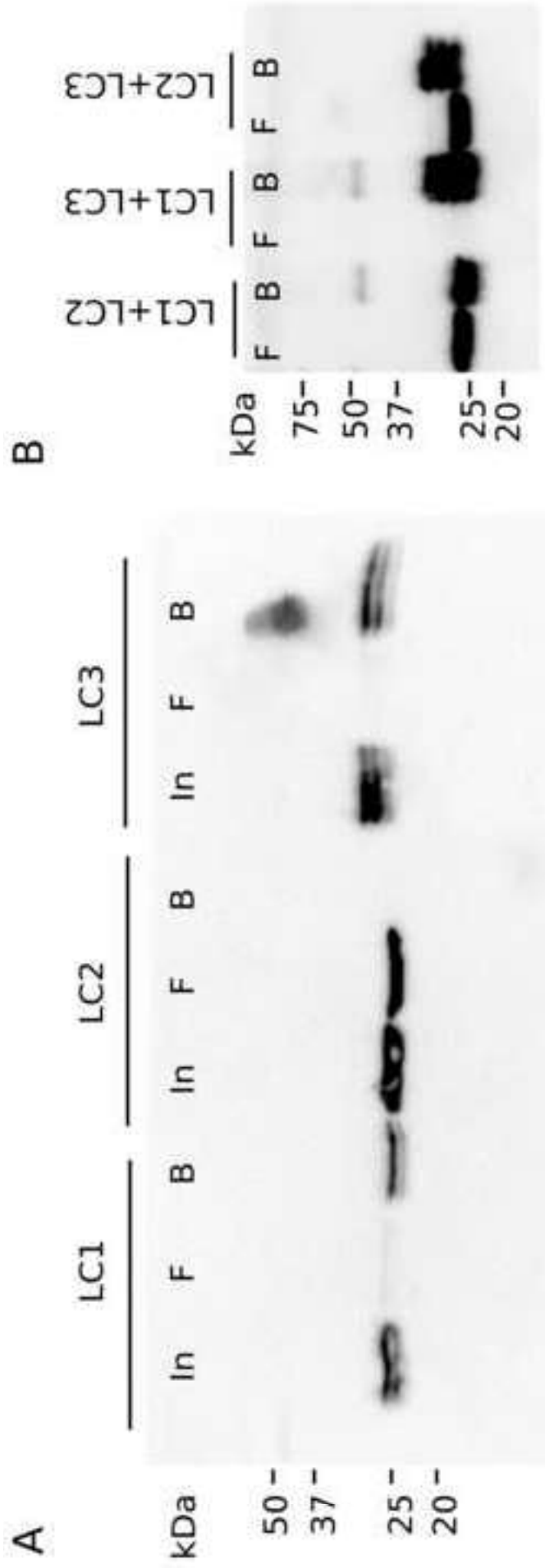531   *Biol Chem*, 278: 26319-22.
532 Wu, J., and M. Filutowicz. 1999. 'Hexahistidine (His6)-tag dependent protein dimerization: a cautionary
533   tale', *Acta Biochim Pol*, 46: 591-9.
534 Zaidman-Remy, A., M. Herve, M. Poidevin, S. Pili-Floury, M. S. Kim, D. Blanot, B. H. Oh, R. Ueda, D.
535   Mengin-Lecreulx, and B. Lemaitre. 2006. 'The Drosophila amidase PGRP-LB modulates the
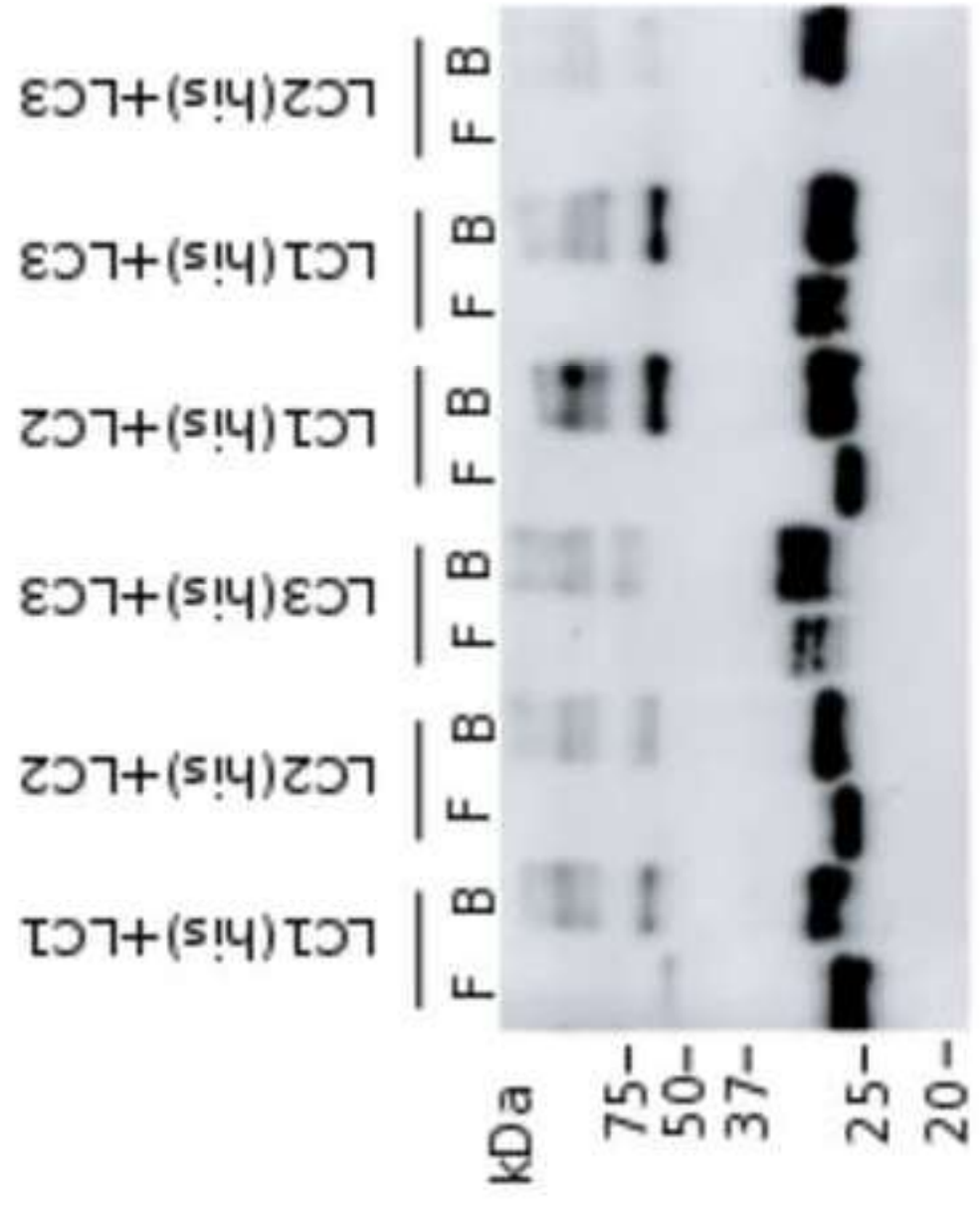536   immune response to bacterial infection', *Immunity*, 24: 463-73.
537

Figure 1

Click here to access/download;Figure;Fig_1.png

Figure 2

Figure 3

Figure 4